Bioconjugate Chemistry

Editors' Choice
Open Access

pubs.acs.org/bc

Article

Supramolecular Biohybrid Construct for Photoconversion Based on a Bacterial Reaction Center Covalently Bound to Cytochrome *c* by an Organic Light Harvesting Bridge

Gabriella Buscemi, Massimo Trotta, Danilo Vona, Gianluca M. Farinola, Francesco Milano,* and Roberta Ragni*

Cite This: *Bioconjugate Chem.* 2023, 34, 629–637

Read Online

ACCESS | Metrics & More | Article Recommendations | Supporting Information

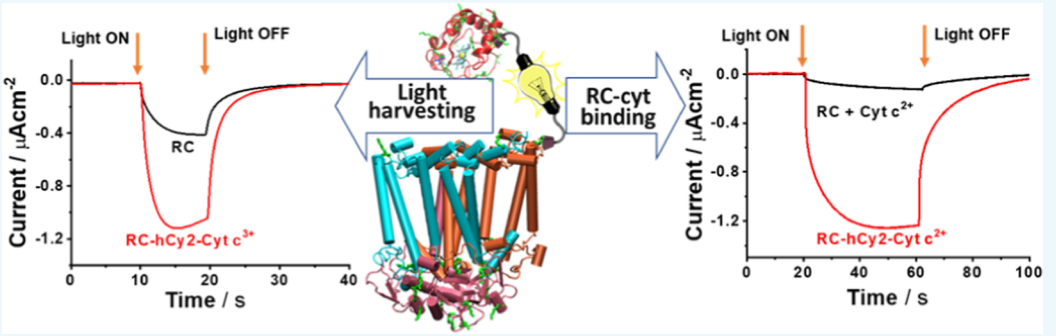

ABSTRACT: A supramolecular construct for solar energy conversion is developed by covalently bridging the reaction center (RC) from the photosynthetic bacterium *Rhodobacter sphaeroides* and cytochrome *c* (Cyt *c*) proteins with a tailored organic light harvesting antenna (hCy2). The RC-hCy2-Cyt *c* biohybrid mimics the working mechanism of biological assemblies located in the bacterial cell membrane to convert sunlight into metabolic energy. hCy2 collects visible light and transfers energy to the RC, increasing the rate of photocycle between a RC and Cyt *c* that are linked in such a way that enhances proximity without preventing protein mobility. The biohybrid obtained with average 1 RC/10 hCy2/1.5 Cyt *c* molar ratio features an almost doubled photoactivity versus the pristine RC upon illumination at 660 nm, and ∼10 times higher photocurrent versus an equimolar mixture of the unbound proteins. Our results represent an interesting insight into photoenzyme chemical manipulation, opening the way to new eco-sustainable systems for biophotovoltaics.

INTRODUCTION

Research of eco-sustainable methods for solar energy conversion based on renewable and/or biocompatible materials has a key role to fulfill current mankind needs,[1−3] preserving natural ecosystems.

In this frame, nature provides scientists inspiration and sources to build up a new generation of biohybrid machineries capable of collecting sunlight and converting it into other forms of energy. Such conversion indeed occurs in photosynthetic organisms by mechanisms and biomacromolecules optimized in billion years of evolution. The light phase mechanism of photosynthesis in plants, algae, and bacteria is based on a highly efficient interplay of three main biological entities: (1) the light harvesting complex proteins that funnel the collected excitation energy to (2) a photochemical core [reaction center (RC)] that generates a photoinduced charge separation and is capable to interact with (3) small electron carriers such as a water soluble electron donor (cytochrome) and a membrane bound electron acceptor (ubiquinone) that, respectively, fuel redox processes in the dark photosynthesis phase.[4]

This interplay is very well characterized in photosynthetic bacteria, such as the purple non-sulfur *Rhodobacter (Rb.) sphaeroides* R26, where it efficiently occurs thanks to the bacterial membrane geometry that forms deep invaginations or even closed vesicles, confining the cytochrome (Cyt c_2) in close proximity of RC, thus allowing their optimal interaction even with 1:1 molar ratio.[5,6] The RC (Scheme 1a) is composed of three subunits enclosing a series of cofactors responsible for the protein photoactivity. Upon direct or light harvesting (LH1)-mediated photoexcitation, a cascade electron transfer is

Received: November 11, 2022
Revised: January 13, 2023
Published: March 10, 2023

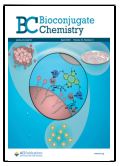

Scheme 1. (a) Simplified Sketch of the Biohybrid with hCy2 Bound to RC (PDB ID: 2J8C[33]) and Cyt *c* (PDB ID: 1hrc[34]); hCy2 is not Depicted in Scale with the Proteins; hCy2 Binds Cyt *c* to One of Its Lysine Residues (Blue Spheres) and RC to at Least One of the Three Lysine Residues Next to the Docking RC Periplasmic Site (Orange Spheres); Further hCy2 Molecules (Not Shown for Clarity) Bind RC in the Cytoplasmic Side to the Lysine Residues Depicted as Green Spheres; Energy and Electron Transfer Processes Occurring by Photoexcitation with Visible Light are Also Depicted: The Antenna Absorbs Visible Light and Transfers NIR Light to the RC Dimer that Transfers an Electron to the UQ_{10} Molecule in the Q_B Pocket; Cyt c^{2+} Reduces the Oxidized Dimer; a Second Photon Absorption Results in the Full Reduction of Semiquinone in Q_B to $UQ_{10}H_2$ Upon Proton Uptake; The Cofactors Represented are the Following: Dimeric Bacteriochlorophyll (Red), Bacteriochlorophyll (Yellow), Bacteriopheophytins (Orange), and Ubiquinone (Purple); (b) Absorption (Black) and Emission (Red) Spectra of hCy2 in $H_{10}L_{0.2}$; (c) Absorption Spectrum of the Biohybrid in $H_{10}L_{0.2}$

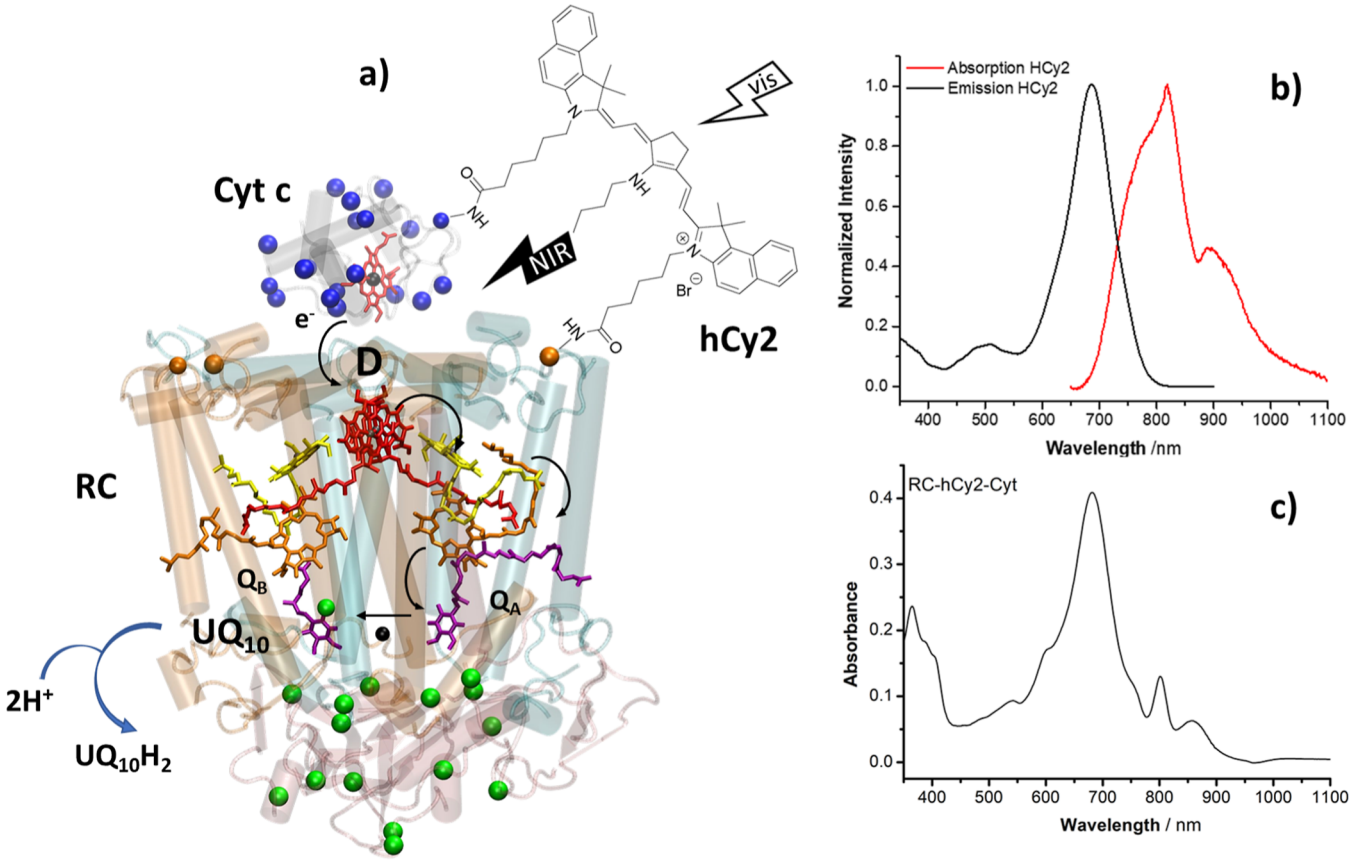

triggered leading to the $D^+Q_B^-$ charge separated state, where D is a dimer of bacteriochlorophylls (represented in red) and Q_B is a ubiquinone-10 (UQ_{10}) molecule (represented in purple) sitting in the Q_B pocket.[7,8] The unitary quantum yield of this process and the remarkably long lifetime of the final state (1−3 s)[9] make bacterial RCs appealing for applications in solar energy conversion. Cyt c_2 reduces D^+ in the μs timescale and a second photon absorption promotes the formation of $UQ_{10}H_2$ molecule by proton uptake from the cytoplasm, contributing to the generation of a transmembrane proton gradient (Scheme 1a).

The above described physiological process, namely, known as RC photocycle promoting a photoinduced uphill redox reaction, provides a mechanism extensively investigated and applied in bioelectronic devices.[10−14]

However, the biological complexity and non-covalent interactions among LH1, RC, and Cyt c_2 are not fully profitable for their application outside the living bacterium cells. Moreover, contrary to RC and Cyt c_2 that can be easily handled after isolation, the use of LH1 suffers from some issues related to both lability of isolated LH1-RC complexes and limited LH1 light collection in the visible range, resulting in enhanced RC absorption cross section only in the near infrared (NIR).[15] On this ground, among possible approaches to enhance the RC cross-section,[16−18] in our previous works, we demonstrated that bioconjugation of suitable organic antenna molecules to the RC is a profitable strategy to generate a stable system with enhanced RC photoactivity in the visible spectral region where the native RC does not efficiently absorb.[19−21]

In this work, we would provide a proof of the concept that it is possible to develop a system with higher photocurrent generation efficiency (Scheme 1a) that is based on stable covalent binding of a tailored bifunctional organic antenna to both RC and horse heart cytochrome *c* (Cyt *c*, used instead of the native Cyt c_2 due to its broad commercial availability and handy processability). Such supramolecular assembly is designed to be capable of collecting sunlight by the antenna, transferring energy to the RC and performing a photocycle with the linked Cyt *c* faster than that occurring when RC and Cyt *c* are not covalently connected. Moreover, this biohybrid machinery has far lower complexity and bulkiness versus the natural RC-LH1-Cyt c_2 assembly, still retaining full activity of the proteins and higher stability in a non-physiological environment.

https://doi.org/10.1021/acs.bioconjchem.2c00527
Bioconjugate Chem. 2023, 34, 629−637

To the best of our knowledge, such a solar energy conversion supramolecular machinery has not been designed and explored so far. Indeed, literature mainly shows studies of possible applications in photoelectrochemical cells of mixtures of unbound RC and Cyt *c* exploiting their natural interaction.[22−24] The rare studies reporting a covalent bond between Cyt *c* and RC aimed only to investigate the docking interactions and the interprotein binding site. In this case, the proteins were covalently bound either by direct conjugation of their carboxyl and amino groups on surface-exposed amino-acidic residues[25] or by a flexible linker without photoactive functions.[26,27]

Here, we report the synthesis and characterization of the RC-hCy2-Cyt *c* covalent supercomplex where a heptamethine cyanine dye (hCy2) acts both as a visible light harvesting antenna and as a linker bridging two proteins. The biohybrid obtained with average 1 RC/10 hCy2/1.5 Cyt *c* molar ratio features 100% photoactivity increase upon illumination at 660 nm versus the pristine RC, and ∼10 times higher photocurrent generation efficiency versus an equimolar mixture of the unbound proteins.

RESULTS AND DISCUSSION

Chemical Design of hCy2. For the biohybrid design, we have focused attention on a molecular dye (hCy2 in Scheme S1) with a heptamethine cyanine structure[28,29] because it can act simultaneously as a linker and light harvesting antenna, fulfilling the following requirements: (1) high extinction coefficient in the visible (400−700 nm) range, where RC has weak absorption bands; (2) large Stokes shift to minimize self-absorption; (3) high emission quantum yield in the NIR (700−900 nm) region, where RC efficiently absorbs; (4) stability in aqueous detergent solution where RC is dissolved; and (5) structural flexibility that would allow linking of RC and Cyt *c* with low steric hindrance to avoid impairing their interaction and activity.

In fact, our previous studies evidenced that a similar heptamethine cyanine dye, with a single bioconjugation site, acts as a very efficient antenna leading to 100% increase of the photoenzyme activity upon visible light (380−680 nm) illumination.[21,30]

Synthesis and Spectroscopic Characterization of hCy2. The desired molecular antenna was obtained from the commercially available Dye847 (see Scheme S1) bearing a central chlorine atom in the heptamethine cyanine backbone and two side alkyl chains ending with a carboxylic group suitable for the bifunctional conjugation with the RC and Cyt *c* proteins upon activation as succinimidyl ester (hCy2-NHS). The commercial Dye847 has intense NIR absorption and emission peaks [λ_{abs} = 863 nm, ε = 332 mM^{-1} cm^{-1}, λ_{em} = 886 nm, quantum yield (QY) = 0.40] in 10 mM HEPES [4-(2-hydroxyethyl)piperazine-1-ethanesulfonic acid], 0.2% LDAO (lauryldimethylamine-*N*-oxide) pH 8.0, ($H_{10}L_{0.2}$ buffer), but limited Stokes shift (23 nm) (Figure S1a,b, black lines).

hCy2 was synthesized by nucleophilic substitution of the central chlorine atom of Dye847 with butylamine as detailed in the Experimental Section. Replacing the central chlorine atom of Dye847 with an amino group is a very straightforward method to induce a large Stokes shift (134 nm) due to a significant hypsochromic shift of the absorption peak (λ_{abs} = 686 nm, ε = 88 ± 10 mM^{-1} cm^{-1}) and a moderate hypsochromic shift in the emission spectrum (λ_{em} = 820 nm, QY = 0.29, Scheme 1b and Figure S1a,b, red lines). This spectroscopic behavior is ascribable to an excited-state intramolecular charge transfer between the amino donor and the cyanine acceptor units.[29,31]

Having good solubility in water, a broad and intense absorption in the visible range, emission overlapping the main RC absorption peaks in the NIR, and two binding groups on flexible alkyl chains, hCy2 was used as photoactive linker between RC and Cyt *c*, upon activation of its carboxyl groups as succinimidyl esters (leading to hCy2-NHS) and bioconjugation with $-NH_2$ lysine residues of proteins (see the Experimental Section and Scheme S2).

The biohybrid was obtained suspending the two proteins in detergent solution to favor their physiological docking interaction in the periplasmic RC side. The subsequent addition of the antenna favors its function to connect one of the RC periplasmic lysine residues to one of the Cyt *c* lysine groups. Indeed, the average distance of the two binding sites in hCy2-NHS estimated as ∼20 Å is not long enough to anchor the antenna to a pair of lysines of the RC periplasmic surface because it is possible to estimate the distances between these lysines as it follows: 56 Å between L82 and M110; 47 Å between L82 and L268; and 28 Å between M110 and L268. Moreover, the flexibility of the hexyl chains of the organic antenna is expected to not hinder the physiological docking interaction of RC and Cyt *c*.

Synthesis and Characterization of RC-hCy2-Cyt Biohybrid. For the synthesis of the biohybrid, to favor the bioconjugation of Cyt *c* by the hCy2 bridge in proximity of the RC dimer, we adapted a synthetic procedure used by Rosen et al., in a study aimed to identify the docking site between the two proteins, in which their binding occurs in the M and L subunits, and is prevented in the H subunit.[26] In fact, the bioconjugation of Cyt *c* to the H subunit was reported by Ueno et al.[27] to occur only after the introduction of thiol groups to RC. Moreover, as shown by Feher et al.,[32] the RC-Cyt *c* co-complex crystal structure demonstrates a natural tendency of RC and Cyt *c* to interact in the position sketched in Scheme 1a. Hence, our RC-hCy2-Cyt *c* biohybrid was obtained by the one-pot reaction between RC, hCy2-NHS, and Cyt *c* mixed in $H_{10}L_{0.2}$ with 1:25:20 molar ratio. RC and Cyt *c* were first incubated for 10 min, then hCy2-NHS was added to the mixture (final concentrations: RC 10 μM, hCy2 200 μM, Cyt *c* 200 μM) and incubated for 1 h in the dark at room temperature (Scheme S2). The biohybrid was eventually purified by size exclusion chromatography. UV−vis−NIR absorption spectroscopy was used to both detect its presence in the eluted fractions (Scheme 1c and Figure S2a) and quantify the RC/hCy2/Cyt *c* molar ratio (Figure S2b).

RC concentration was obtained by the absorption peak at 802 nm (ε = 288 mM^{-1} cm^{-1}),[35] where there is minimal contribution of both hCy2 and Cyt *c*. The corresponding RC absorption spectrum was then subtracted from that of the bioconjugate. This allows to quantify both the hCy2 and Cyt *c* concentrations from the absorption peaks at 686 and 410 nm (ε = 106 mM^{-1} cm^{-1}),[36] respectively, where the two contributions are separated. Hence, a 1 RC/10 hCy2/1.5 Cyt *c* binding ratio was estimated.

The high number of bound hCy2 molecules is likely due to their good solubility in water that allows bioconjugation not only to the 3 RC lysines next to the Cyt *c* docking site (M110, L83, and L268, orange spheres in Scheme 1a) but also to the 16 lysines on the opposite side of the membrane (green spheres in Scheme 1a).[37]

https://doi.org/10.1021/acs.bioconjchem.2c00527
Bioconjugate Chem. 2023, 34, 629−637

As shown in the absorption spectra of Figure S2a, the RC-hCy2-Cyt *c* biohybrid was isolated as the first fraction eluted by size exclusion chromatography, whereas a mixture of unbound Cyt *c* and hCy2 used in excess was subsequently eluted and removed. The 1:1.5 RC/Cyt *c* binding ratio suggests that in the first eluted fraction, there is a mixture of biohybrids bearing one or two linked Cyt *c*-hCy2 moieties per one RC photoenzyme. Because the 1:1 co-complex RC/Cyt spontaneously forms upon incubation, it is expected that at least one bioconjugation of the hCy2-Cyt *c* moiety to the RC occurs in the natural docking site of Cyt *c* nearby the RC periplasmic side. Figure S3 shows the emission spectrum of the biohybrid strongly resembling that of hCy2, with a slight broadening of the emission band at low wavelengths.

Sodium dodecyl sulfate polyacrylamide gel electrophoresis (SDS-PAGE) of biohybrid loaded at the same concentration of native RC revealed that all RC subunits are involved in the bioconjugation reaction due to the very low intensity of the unreacted H, L, and M bands[38,39] of the biohybrid and the appearance of a series of bands at higher molecular weights (see Supporting Information, Figure S4 and Table S1). Although being a proof of successful bioconjugation, uncertainties on molecular weights due to the different amounts of SDS that can be bound on hydrophobic/hydrophilic subunits[40] and the non-negligible weight of the antenna linker (~800 Da) versus the protein weights, prevent any assignment of the additional biohybrid bands to specific structures.

Photoactivity of RC-hCy2-Cyt *c* Biohybrid. RC-hCy2-Cyt *c* fully retains the photoactivity of RC in generating charge separated states, as shown by the similarity of absorbance changes profiles versus time recorded at 860 nm upon flashlight excitation for both isolated RC and the biohybrid bearing Cyt *c* in the oxidized state (Figure 1, black and purple traces respectively). In particular, RC dimer photobleaching and subsequent dark decay due to the charge recombination process were observed at 860 nm in the $H_{10}L_{0.2}$ buffer.

The dark decay was fitted to a biexponential function, and the obtained kinetic parameters are reported in Table S2. The first exponential (fast decay with A_F amplitude and k_F kinetic constant) refers to the charge recombination from the $D^+Q_A^-$ state, and the second exponential (slow decay with A_S amplitude and k_S kinetic constant) refers to the charge recombination from the $D^+Q_B^-$ state. In the isolated RC, the fast phase accounts for more than 70% of the overall signal, indicating that the Q_B site is mainly inactive, as expected by the high LDAO concentration that partially extracts the UQ_{10} from the Q_B pocket. Moreover, the A_S value for RC-hCy2-Cyt c^{3+} is lower likely because a further amount of UQ_{10} is extracted from the Q_B-site during the chromatographic purification of the biohybrid. As an indirect proof that hCy2 bridges the Cyt *c* next to the RC dimer, we explored the effect of ascorbate addition on the biohybrid transient absorption profile. Ascorbate was added at 100 μM concentration, suitable to fully reduce Cyt c^{3+} avoiding the direct electron donation by ascorbate to the oxidized RC dimer, as demonstrated by the red trace in Figure 1. Upon addition of ascorbate to the biohybrid, a drastic reduction of the overall signal amplitude was observed, indicating that the reduction of D^+ by the Cyt c^{2+} is too fast to be recorded by our instrumental setup. This experimental evidence suggests that, in the obtained biohybrid, hCy2 likely clamps the two proteins with Cyt *c* in close proximity of RC dimer. Indeed, a similar output arises from the same experiment carried out using a mixture of RC and Cyt *c* (1:1.5 molar ratio) in the presence of ascorbate (Figure 1, blue trace) that demonstrates the strong tendency of the two proteins to spontaneously arrange in the docked configuration. Moreover, an intermolecular photoinduced electron transfer from Cyt *c* to the dimer of another biohybrid molecule is not expected to efficiently occur because the steric hindrance would impair their proper approach.

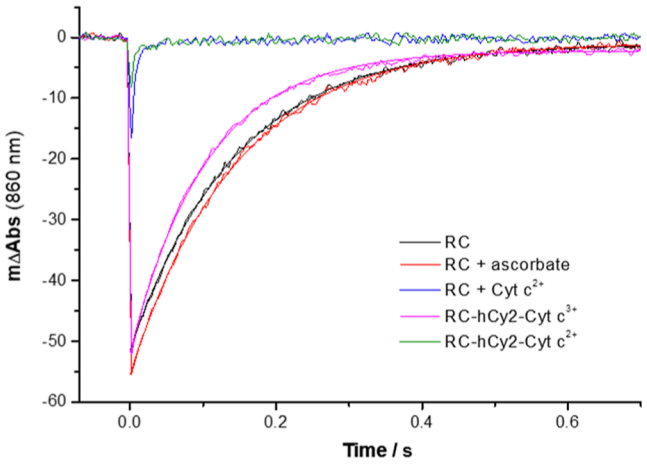

Figure 1. Absorbance changes in $H_{10}L_{0.2}$ recorded at 860 nm for RC alone (black), RC mixed with ascorbate (red), RC mixed with Cyt c^{2+} 1:1.5 in the presence of ascorbate (blue), RC-hCy2-Cyt c^{3+} (magenta), and RC-hCy2-Cyt c^{2+} (green). When needed, 100 μM ascorbate was used to reduce Cyt *c*. RC was 0.6 μM in all samples.

To better envisage the possible arrangement of bound hCy2-Cyt *c* moieties with respect to the dimer, the transient absorption was also recorded illuminating both the biohybrid and a RC-Cyt *c* mixture (same 1:1.5 molar ratio as in the biohybrid) with a series of saturating flashes every 50 ms (Figure 2 panels a–d, where red traces are for the biohybrid and black traces are for the mixture). When Cyt *c* is oxidized, charge recombination occurs only partially because D^+ is re-excited before its decay to D (Figure 2a). In the presence of 100 μM ascorbate (Figure 2b), Cyt c^{3+} is totally reduced to Cyt c^{2+}, and upon the first flash pulse, Cyt c^{2+} rapidly reduces all the photogenerated D^+. In the subsequent flashes and more evidently from the third one, the D^+ signal progressively increases as a consequence of Cyt c^{2+} oxidation. This result suggests that the average 1.5 Cyt *c* molecules in the biohybrid are linked in proximity of the dimer, allowing its fast reduction in the first two pulses (red trace).

A further proof of this proximity was gained monitoring the Cyt *c* oxidation state variation at 550 nm upon photoinduced electron transfer to D^+ (Figure 2c,d). Indeed, at 550 nm, the difference in absorbance between Cyt c^{2+} (higher) and Cyt c^{3+} (lower) is maximum (Figure S2b blue and red traces, respectively). The transient absorption was again detected exciting the biohybrid with saturating flashes every 50 ms. Also in this case, for RC-hCy2-Cyt c^{3+}, only the absorbance changes due to D/D^+ are observed (Figure 2c) because Cyt c^{3+} cannot participate to the process. Conversely, in the presence of ascorbate (Figure 2d), the recorded absorbance changes reveal the Cyt c^{2+} to Cyt c^{3+} redox transition.[41]

As a confirmation that one or two Cyt *c* molecules are located nearby the dimer, the first two flashes provide square shaped responses, due to the full reduction of D^+ by two

https://doi.org/10.1021/acs.bioconjchem.2c00527
Bioconjugate Chem. 2023, 34, 629–637

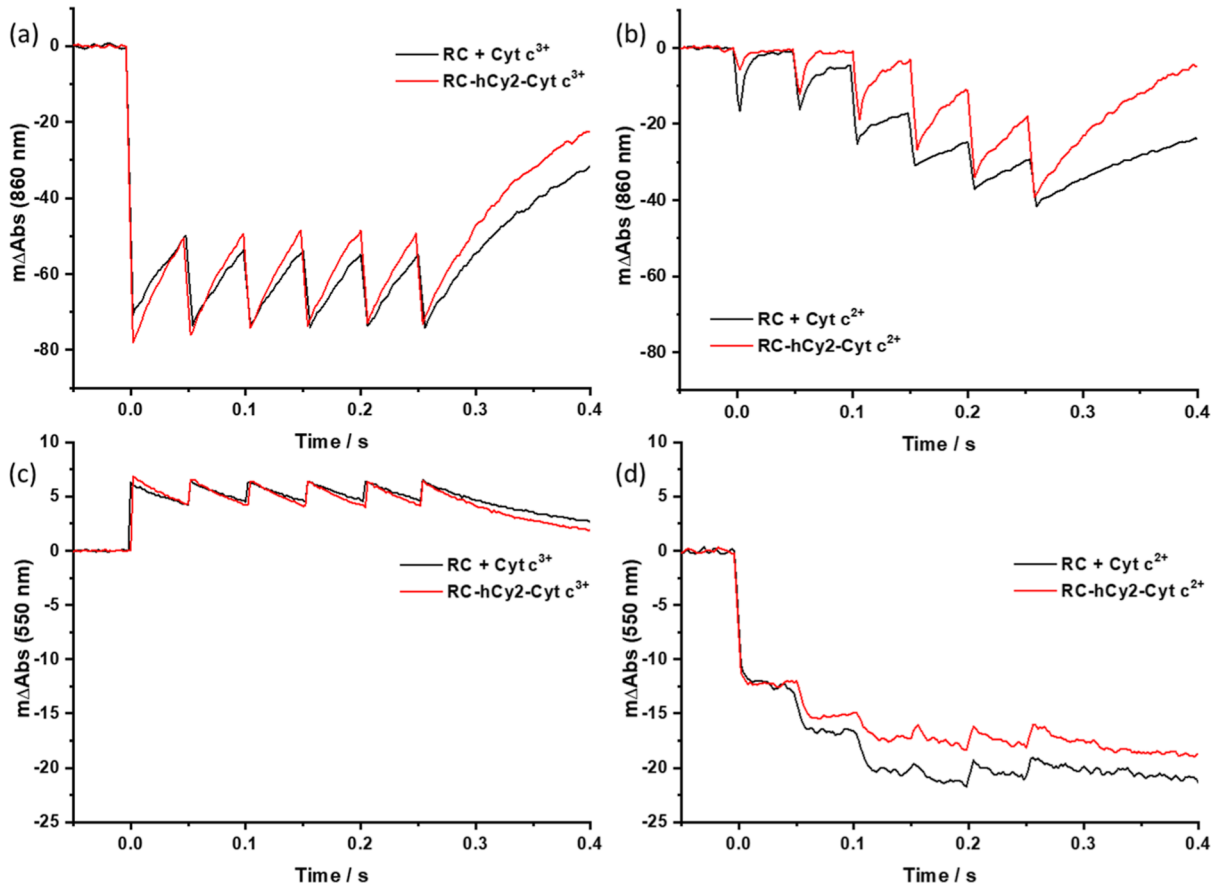

Figure 2. Absorbance changes for (a) RC mixed with Cyt c^{3+} 1:1.5 (black) and RC-hCy2-Cyt c^{3+} (red) recorded at 860 nm, (b) RC mixed with Cyt c^{2+} 1:1.5 (black) and RC-hCy2-Cyt c^{2+} (red) recorded at 860 nm, (c) RC mixed with Cyt c^{3+} 1:1.5 (black) and RC-hCy2-Cyt c^{3+} (red) recorded at 550 nm, and (d) RC mixed with Cyt c^{2+} 1:1.5 (black) and RC-hCy2-Cyt^{2+} (red) recorded at 550 nm. RC = 0.8 μM in $H_{10}L_{0.2}$ and dQ 50 μM in all cases. All samples were excited with six flashes every 50 ms.

nearby Cyt c^{2+}, while in the subsequent flashes the D^+ contribution gradually appears.

The signal intensity in Figure 2d also allows us to estimate the amount of Cyt c^{2+} oxidized at each flash. Considering that the Cyt c differential molar extinction coefficient is 18.7 mM^{-1} cm^{-1}[36] and that the RC concentration is 0.8 μM, a signal of 15 mA is predictable if RC fully oxidates Cyt c^{2+} after the first flash. The measured 12.5 mA signal, despite different from 15 mA, is however coherent with that expected because the monochromator slit width of our instrumental setup has a bandpass slightly larger than the very sharp Cyt c^{2+} peak at 550 nm, this lowering the signal value. Moreover, a signal of 12.5 mA results when an excess Cyt c^{2+} is mixed in a 0.8 μM RC solution as a control test (Figure S5). Applying this instrumental correction, the total amount of Cyt c oxidized by the RC is 1.16 μM, that corresponds to 1.45 Cyt c/RC molar ratio, in good agreement with the ratio found by steady state spectroscopy.

The same experiment carried out for the mixture of unbound RC and Cyt c at 1:1.5 molar ratio leads to a very similar pattern, again confirming the strong affinity of RC and Cyt c.

hCy2 Light Harvesting Antenna Effect. The antenna effect of hCy2 was first evaluated comparing the efficiency of generation of $D^+Q_A^-$ charge separated state by 1 μM solutions of RC and RC-hCy2-Cyt c^{3+} in $H_{10}L_{0.2}$ buffer, upon continuous photoexcitation at 660 ± 10 nm, close to the maximum absorption of the dye and minimum absorption of the photoenzyme. Cyt c in the biohybrid was completely oxidized to avoid any interference with the assay. $D^+Q_A^-$ concentration was evaluated recording the absorbance change at 860 nm using the differential molar extinction coefficient $\Delta\varepsilon$ = 112 mM^{-1} cm^{-1}.[35] As shown in Figure 3a, 1.9-fold increase of $D^+Q_A^-$ concentration was recorded for RC-hCy2-Cyt c^{3+} versus RC, confirming the light harvesting and energy transfer abilities of the antenna.

Further evidence of the antenna effect was provided measuring the efficiencies of photocurrent generation upon selective excitation at 660 ± 10 nm of 0.1 μM solutions of RC and RC-hCy2-Cyt c^{3+} in the $H_{10}L_{0.2}$ buffer. In particular, the experiments were carried out in a three-electrode electrochemical cell (see electrochemical measurements in the Supporting Information). To reproduce in vitro the bacterial RC photocycle occurring in vivo, decylubiquinone (dQ, 200 μM) and ferrocenemethanol (FcMeOH, 300 μM) were used as the electrochemical mediators[42,43] instead of the physiological electron acceptor ubiquinone-10 (UQ_{10}) and electron donor Cyt c_2, respectively. A scheme of the photochemical and electrochemical reactions occurring in the cell is provided in Figure S5a. The net reaction occurring under illumination is the dQ reduction to dQH_2 and FcMeOH oxidation to $FcMeOH^+$. Also in this case, Cyt c in the biohybrid was completely oxidized to avoid its contribution as electron donor and to ascribe the different photocurrent outputs for RC and

https://doi.org/10.1021/acs.bioconjchem.2c00527
Bioconjugate Chem. 2023, 34, 629−637

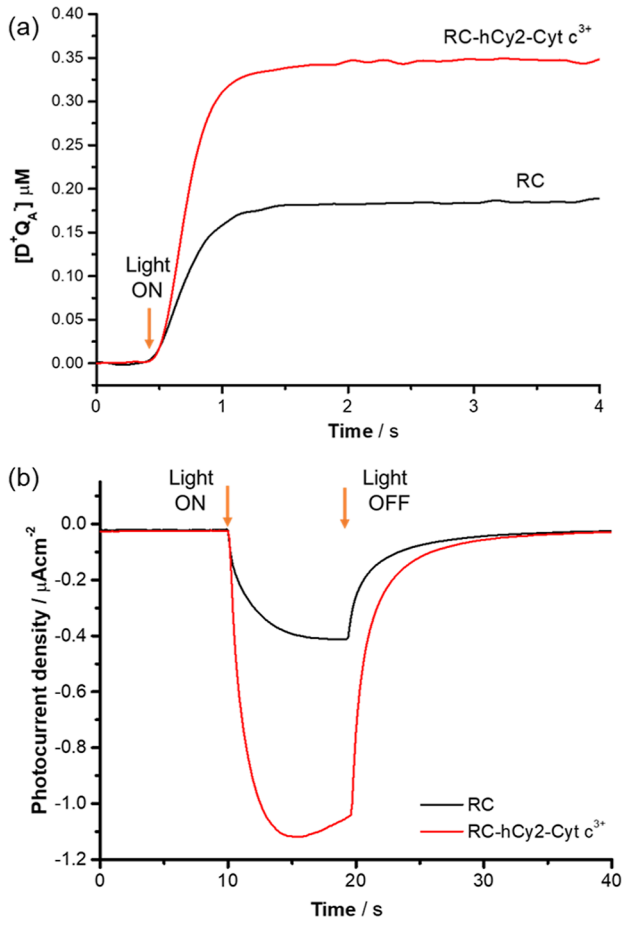

Figure 3. (a) Concentration of the charge separated state $D^+Q_A^-$ detected in $H_{10}L_{0.2}$ at 860 nm for native RC (black) and RC-hCy2-Cyt c^{3+} (red). Data refer to 1 μM RC illuminated with sub-saturating light at 660 nm. (b) Photocurrents detected in phosphate buffer 100 mM pH 6.9 at −0.1 V vs Ag/AgCl, with excitation at 660 nm, 200 μM dQ, 300 μM FcMeOH, 0.1 μM RC (black), and 0.1 μM RC-hCy2-Cyt c^{3+} (red).

biohybrid to the sole antenna effect. Chronoamperometric profiles (Figure 3b) clearly show that, as an effect of the antenna, the cathodic photocurrent (due to $FcMeOH^+$ reduction at the WE) from the biohybrid is 2.8-fold higher than that from RC.

hCy2 Bridging Effect. Nevertheless, all the experiments reported so far, are not exhaustive to really evidence that the macromolecular RC-hCy2-Cyt *c* biohybrid represents a more effective system for photocurrent generation versus a simple mixture of its unbound protein moieties. For this aim, we eventually compared the photocurrent production capability of 0.1 μM biohybrid versus that of a RC/Cyt *c* mixture at the same concentrations.

Experiments were performed with the same setup used to evaluate the antenna effect (Figure S5b). In this case, the photocycle was sustained directly exciting the RC at 860 nm, with the aim to exclude any interference of the antenna. For comparison, we tested the direct Cyt *c* effect as the electron donor in the biohybrid and in the mixture with RC. In both cases dQ was added as the electron acceptor. As shown in Figure 4, when the two proteins are covalently bridged by the flexible hCy2 linker, a remarkable (~10-fold) increase of

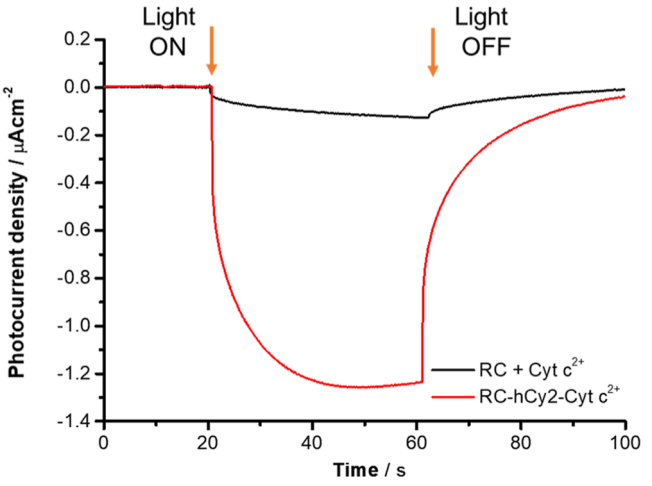

Figure 4. Photocurrents detected at λ_{ex} 860 nm and −0.1 V vs Ag/AgCl, for 0.1 μM RC mixed with 0.15 μM Cyt c^{2+} (black) and 0.1 μM RC-hCy2-Cyt c^{2+} (red). 200 μM dQ and 10 mM potassium ferrocyanide were used as redox mediators. All measurements were performed in phosphate buffer 100 mM pH 6.9.

photocurrent density is observed (up to ~1.2 $\mu A/cm^2$) with respect to the RC/Cyt *c* mixture.

Moreover, the 10-fold photocurrent increase, combined with the previously shown antenna effect, strengthens the effectiveness of the supramolecular assembly of RC-hCy2-Cyt *c* for biophotoconversion. In fact, on the one side, it overperforms a mixture of free RC and Cyt *c* proteins despite their mutual extreme affinity and, on the other side, it benefits of the light harvesting capability of the tailored organic antenna linker.

CONCLUSIONS

In conclusion, we provide a supramolecular covalent assembly taking inspiration from the bacterial confinement of the RC photoenzyme responsible for efficient conversion of photons into charge separated states and the Cyt c_2 electron carrier that is prefixed to reduce the oxidized RC dimer triggering the process that eventually produces the transmembrane proton gradient. The biohybrid has been conceived to have a quite simple architecture in which a tailored organic bifunctional antenna hCy2 bridges the RC and Cyt *c* proteins overcoming the issues of processability of the bacterial light harvesting complex LH1 that naturally surrounds the RC.

Our work clearly demonstrates that the covalent bridging approach does not impair the mutual proteins interaction, while boosting the photocurrent generation of 1 order of magnitude with respect to an equimolar mixture of the unbound proteins. As a further benefit, upon selective illumination at hCy2 absorption maximum, a twofold increase of charge separated state concentration and threefold increase of photocurrent intensity are observed in the biohybrid as the effects of the organic antenna light harvesting.

The antenna-mediated bacterial-protein binding design shown herein for the realization of the RC-hCy2-Cyt *c* biohybrid represents a new route to efficient and ecosustainable materials for solar energy conversion.

EXPERIMENTAL SECTION

Chemicals. HEPES, decylubiquinone (dQ), potassium ferrocyanide, FcMeOH, LDAO, Cytochrome *c* from horse

https://doi.org/10.1021/acs.bioconjchem.2c00527
Bioconjugate Chem. 2023, 34, 629−637

heart (Cyt c^{3+}, i.e., in the oxidized state), and methanol were purchased from Sigma. L-Ascorbic acid sodium salt was purchased from Thermo Fisher Scientific. All reagents and solvents for the synthesis of hCy2 and hCy2-NHS were purchased from Sigma-Aldrich. Dye847 (847 refers to its maximum absorption in methanol) was from Crysta-Lyn Chemical Company (Binghamton, NY, USA). All aqueous solutions were prepared using water purified by the Milli-Q Gradient A-10 system (Millipore, 18.2 MΩ cm, organic carbon content ≤ 4 μg/L). Pre-coated thin-layer chromatography (TLC)-plates RP-18/UV254 by Macherey-Nagel Gmbh & Co with silica gel C-18 layer of 0.15 and 0.25 mm were used for analytical and preparative TLC, respectively. CombiFlash Rf+ chromatograph equipped with a 50 g gold reverse phase C-18 column was used for purification of cyanine molecules. High-resolution mass spectra were recorded by a Shimadzu high-performance liquid chromatography-ion trap-time of flight mass spectrometer (LCMS-IT-TOF). ^{1}H NMR and ^{13}C NMR spectra were recorded at 500 and 125 MHz, respectively, using an Agilent Technologies 500/54 Premium Shielded spectrometer.

Synthesis of the Antenna. *2-((E)-2-((Z)-2-(Butylamino)-3-((Z)-2-(3-(5-carboxypentyl)-1,1-dimethyl-1,3-dihydro-2H-benzo[e]indol-2-ylidene)ethylidene) Cyclopent-1-en-1-yl)-vinyl)-3-(5-carboxypentyl)-1,1-dimethyl-1H-benzo[e]indol-3-ium Bromide (hCy2).* A suspension of Dye847 (0.600 g, 0.7 mmol) and *n*-butylamine (2.12 mL, 21.4 mmol) in dry *N*,*N*-dimethylformamide (DMF) (20 mL) was stirred overnight under a nitrogen atmosphere in the dark at 80 °C. Then, the crude mixture was cooled and DMF was evaporated under vacuum. The residues of solvent and *n*-butylamine were removed washing the crude mixture with water and filtering the solid product in a Buchner funnel. hCy2 was then purified by C-18 column chromatography eluting with a mixture of methanol and water (9:1 v/v). A dark solid was recovered in 27% yield after distillation of the eluent. ^{1}H NMR (500 MHz, CD_3OD): 1.11 (t, *J* = 7.4 Hz, 3H), 1.47−1.56 (m, 2H), 1.57−1.66 (m, 2H), 1.67−1.75 (m, 4H), 1.78−1.89 (m, 4H), 1.90−2.05 (m, 16H), 2.28 (t, *J* = 7.3 Hz, 4H), 3.54−3.58 (m, 2H), 3.66−3.70 (m, 2H), 3.84−3.90 (m, 2H), 3.99−4.08 (m, 4H), 5.7 (d, *J* = 12.7 Hz, 2H), 7.37 (tl, *J* = 8 Hz, 2H), 7.42 (d, *J* = 8.8 Hz, 2H), 7.55 (tl, *J* = 8 Hz, 2H), 7.91 (d, *J* = 8.6 Hz, 4H), 8.02 (d, *J* = 12.7 Hz, 2H), 8.14 (d, *J* = 8.6 Hz, 2H). ^{13}C NMR (125 MHz, CD_3OD): 12.89, 20.07, 22.30, 24.57, 24.99,26.06, 26.25, 26.64, 29.02, 29.30, 31.96, 35.1, 42.48, 60.85, 72.11, 95.78, 109.95, 114.78, 119.11, 121.50, 123.42, 126.96, 128.38, 129.02, 129.61, 129.89, 130.97, 131.06, 140.45, 168.57, 178.23. HRMS: $[M - Br]^+$ *m*/*z* calcd, 806.4891; found, 806.4901.

2-((E)-2-((Z)-2-(Butylamino)-3-((E)-2-(3-(6-((2,5-dioxopyrrolidin-1-yl)oxy)-6-oxohexyl)-1,1-dimethyl-1,3-dihydro-2H-benzo[e]indol-2-ylidene)ethylidene)cyclopent-1-en-1-yl)-vinyl)-3-(6-((2,5-dioxopyrrolidin-1-yl)oxy)-6-oxohexyl)-1,1-dimethyl-1H-benzo[e]indol-3-ium Bromide (hCy2-NHS). hCy2 (0.1 g, 0.11 mmol) and *N*-hydroxysuccinimide (0.13 g, 1.1 mmol) were suspended under a nitrogen atmosphere in dry DMF (5 mL), and a solution of *N*,*N*′-dicyclohexylcarbodiimide (0.28 g, 1.3 mmol) in dry DMF (2 mL) was added. The mixture was stirred for 24 h in the dark, at room temperature, monitoring the reaction by TLC. Then, DMF was evaporated at reduced pressure and room temperature. The crude mixture was dissolved in methanol and *N*,*N*′-dicyclohexylurea was filtered off as a white solid byproduct. hCy2-NHS was then recovered as a dark blue solid by distillation of the solvent and used without further purification.

Synthesis of RC-hCy2-Cyt *c*. RC was isolated from *Rhodobacter sphaeroides* strain R26 according to the literature.[44] The lysine-specific bioconjugation reaction was performed incubating RC and Cyt *c* at 10 and 200 μM final concentrations, respectively, in $H_{10}L_{0.2}$ for 10 min. Then, hCy2-NHS (400 μM in $H_{10}L_{0.2}$) was added reaching final RC/hCy2/Cyt *c* ratio of 1:25:20. The reaction mixture was stirred for 1 h in the dark at room temperature. The biohybrid was purified by size exclusion chromatography (Sephadex G100-superfine) eluting with $H_{10}L_{0.2}$. Absorption spectra were recorded to confirm that the first eluted fraction with higher molecular weight contains the biohybrid, whereas the second one only includes the Cyt *c* excess. The unreacted hCy2-NHS is not eluted during the chromatography, being visible at the head of the column.

SDS-PAGE Gel Electrophoresis. For sodium dodecyl sulfate polyacrylamide gel electrophoresis (SDS-PAGE), a 12% polyacrylamide matrix was used. The samples of marker, RC, and RC-hCy2-Cyt *c* were denatured in dithiothreitol (1% w/v)−SDS (2.5% w/v) solution at 90 °C for 5 min. The same amount of each sample (20 μg) was loaded in each gel well, working in duplicate for RC and RC-hCy2-Cyt *c*. Coomassie brilliant blue was used to stain the proteins bands. A calibration curve was obtained plotting the logarithm of molecular weights of markers bands versus the relative migration distance R_f.

Steady State UV−Vis−NIR Absorption and Fluorescence Emission Spectroscopy. UV−vis−NIR absorption spectra in the range 350−1100 nm were recorded in MeOH or $H_{10}L_{0.2}$ using a Cary 5000 spectrophotometer (Agilent Technologies Inc.-USA). Fluorescence emission spectra of Dye 847 and hCy2 were obtained using a Fluorolog 3 (Horiba Scientific-Kyoto, Japan) fluorescence spectrophotometer equipped with a nitrogen cooled solid-state detector sensitive in the NIR region. Maximum absorption of the samples was set to 0.1 in $H_{10}L_{0.2}$ buffer. Dye 847 was excited at 775 nm and emission was collected in the 800−1200 nm range. HCy2 and RC-hCy2-Cyt *c* were excited at 640 nm and emission was collected in the 650−1200 nm range. Emission and excitation slit apertures were 5 nm and emission grating density was 900 lines/mm with blaze at 950 nm in all cases.

Transient Absorption Measurements. Transient absorption spectra were recorded using a local design kinetic spectrophotometer[45] based on a 50 W QTH lamp, a Jobin Yvon H10 IR monochromator, and a Hamamatsu R928 photomultiplier (Hamamatsu Photonics K.K., Hamamatsu City, Japan). A 250 W QTH lamp was used for continuous light excitation, placed at 90° with respect to the probe beam, and, if needed, optical filters were used to excite samples with specific wavelengths. A digital oscilloscope (Tektronix TKS3200) was used to collect the resulting data. All samples were in $H_{10}L_{0.2}$ with the addition of either 100 μM terbutryn or 50 μM dQ. When needed, 100 μM sodium ascorbate was added to reduce Cyt *c*. Illumination at 660 nm was performed by a 100 W 12 V QTH lamp with a 10 nm bandpass filter giving 8 mW/cm^2 irradiance.

Electrochemical Measurements. The electrochemical measurements were performed using a three-electrode single chamber system, with an Autolab potentiostat PGSTAT 10. An Ag/AgCl microelectrode, a Pt wire and an ITO covered glass slide were used as the reference, the counter and the working

https://doi.org/10.1021/acs.bioconjchem.2c00527
Bioconjugate Chem. 2023, 34, 629−637

electrodes, respectively. The ITO glass slides had ∼10 Ω sq^{-1} surface resistivity, >85% transmittance, and 0.72 cm^2 illuminated area in solution. ITO slides were washed sonicating for 10 min in 5% Hellmanex solution and rinsed with bidistilled water and acetone prior their use. The phosphate buffer 100 mM pH 6.9 was used as the support electrolyte. When Cyt *c* was used as the electron donor, 10 mM potassium ferrocyanide and 200 μM dQ were used as electrochemical mediators. 300 μM FcMeOH was used as electron donor in the presence of Cyt c^{3+}. A bias potential of −0.10 V between the reference and the working electrodes was applied, corresponding to the OCV value in the dark. The light source for the photocurrent generation was a 2.6 W LED emitting at 860 nm with 25 mW/cm^2 irradiance. Illumination at 660 nm was performed by a 100 W 12 V QTH lamp with a 10 nm bandpass filter giving 8 mW/cm^2 irradiance.

■ ASSOCIATED CONTENT

Supporting Information

The Supporting Information is available free of charge at https://pubs.acs.org/doi/10.1021/acs.bioconjchem.2c00527.

Schemes of synthetic reactions leading to hCy2, hCy2-NHS, and RC-hCy2-Cyt *c*; absorption and emission spectra of Dye847, hCy2, and RC-hCy2-Cyt *c*; absorption spectra of fractions eluted from the SEC column during the RC-hCy2-Cyt *c* purification; SDS-PAGE of RC-hCy2-Cyt *c* and relevant table of molecular weights of detected bands; and absorbance changes at 550 nm for a RC/Cyt c^{2+} (1:20) mixture flashed six times every 50 ms in the presence of dQ excess (PDF)

■ AUTHOR INFORMATION

Corresponding Authors

Francesco Milano − *Istituto di Scienze delle Produzioni Alimentari, Consiglio Nazionale delle Ricerche (CNR-ISPA), 73100 Lecce, Italy;* orcid.org/0000-0001-5453-2051; Email: francesco.milano@cnr.it

Roberta Ragni − *Dipartimento di Chimica, Università degli Studi di Bari Aldo Moro, 70126 Bari, Italy;* orcid.org/0000-0002-0451-7096; Email: roberta.ragni@uniba.it

Authors

Gabriella Buscemi − *Dipartimento di Chimica, Università degli Studi di Bari Aldo Moro, 70126 Bari, Italy*

Massimo Trotta − *Istituto per i Processi Chimico Fisici, Consiglio Nazionale delle Ricerche (CNR-IPCF), 70126 Bari, Italy;* orcid.org/0000-0002-8220-4597

Danilo Vona − *Dipartimento di Chimica, Università degli Studi di Bari Aldo Moro, 70126 Bari, Italy*

Gianluca M. Farinola − *Dipartimento di Chimica, Università degli Studi di Bari Aldo Moro, 70126 Bari, Italy;* orcid.org/0000-0002-1601-2810

Complete contact information is available at: https://pubs.acs.org/10.1021/acs.bioconjchem.2c00527

Author Contributions

The manuscript was written through contributions of all authors. All authors have given approval to the final version of the manuscript.

Funding

This work was supported by H2020-MSCA-ITN-2019 project 860125-BEEP (Bioinspired and bionic materials for enhanced photosynthesis).

Notes

The authors declare no competing financial interest.

■ ACKNOWLEDGMENTS

This work is dedicated to Professor Roberta Musio, keen scientist and beloved friend. The research group of Professor Ludovico Valli is acknowledged for kindly providing the Fluorolog 3 instrumental setup for fluorescence measurements.

■ REFERENCES

(1) Fang, X.; Kalathil, S.; Reisner, E. Semi-biological approaches to solar-to-chemical conversion. *Chem. Soc. Rev.* **2020**, *49*, 4926−4952.

(2) McCormick, A. J.; Bombelli, P.; Bradley, R. W.; Thorne, R.; Wenzel, T.; Howe, C. J. Biophotovoltaics: oxygenic photosynthetic organisms in the world of bioelectrochemical systems. *Energy Environ. Sci.* **2015**, *8*, 1092−1109.

(3) Kamran, M. Bioenergy. *Renewable Energy Conversion Systems*; Kamran, M., Fazal, M. R., Eds.; Academic Press, 2021; pp 243−264.

(4) Blankenship, R. E. *Molecular Mechanisms of Photosynthesis*; Blackwell Science Ltd.: Oxford, 2002.

(5) Joliot, P.; Verméglio, A.; Joliot, A. Supramolecular organization of the photosynthetic chain in chromatophores and cells of Rhodobacter sphaeroides. *Photosynth. Res.* **1996**, *48*, 291−299.

(6) Scheuring, S.; Nevo, R.; Liu, L. N.; Mangenot, S.; Charuvi, D.; Boudier, T.; Prima, V.; Hubert, P.; Sturgis, J. N.; Reich, Z. The architecture of Rhodobacter sphaeroides chromatophores. *Biochim. Biophys. Acta* **2014**, *1837*, 1263−1270.

(7) Feher, G.; Allen, J. P.; Okamura, M. Y.; Rees, D. C. Structure and function of bacterial photosynthetic reaction centres. *Nature* **1989**, *339*, 111−116.

(8) Deisenhofer, J.; Michel, H. The Photosynthetic Reaction Center from the Purple Bacterium Rhodopseudomonas viridis. *Science* **1989**, *245*, 1463−1473.

(9) Nagy, L.; Milano, F.; Dorogi, M.; Agostiano, A.; Laczkó, G.; Szebényi, K.; Váró, G.; Trotta, M.; Maróti, P. Protein/lipid interaction in the bacterial photosynthetic reaction center: Phosphatidylcholine and phosphatidylglycerol modify the free energy levels of the quinones. *Biochemistry* **2004**, *43*, 12913−12923.

(10) Milano, F.; Punzi, A.; Ragni, R.; Trotta, M.; Farinola, G. M. Photonics and Optoelectronics with Bacteria: Making Materials from Photosynthetic Microorganisms. *Adv. Funct. Mater.* **2019**, *29*, 1805521.

(11) Ravi, S. K.; Udayagiri, V. S.; Suresh, L.; Tan, S. C. Emerging Role of the Band-Structure Approach in Biohybrid Photovoltaics: A Path Beyond Bioelectrochemistry. *Adv. Funct. Mater.* **2017**, *28*, 1705305.

(12) Di Lauro, M.; Gatta, S.; Bortolotti, C. A.; Beni, V.; Parkula, V.; Drakopoulou, S.; Giordani, M.; Berto, M.; Milano, F.; Cramer, T.; Murgia, M.; Agostiano, A.; Farinola, G. M.; Trotta, M.; Biscarini, F. A Bacterial Photosynthetic Enzymatic Unit Modulating Organic Transistors with Light. *Adv. Electron. Mater.* **2019**, *6*, 1900888.

(13) Lo Presti, M.; Giangregorio, M. M.; Ragni, R.; Giotta, L.; Guascito, M. R.; Comparelli, R.; Fanizza, E.; Tangorra, R. R.; Agostiano, A.; Losurdo, M.; Farinola, G. M.; Milano, F.; Trotta, M. Photoelectrodes with Polydopamine Thin Films Incorporating a Bacterial Photoenzyme. *Adv. Electron. Mater.* **2020**, *6*, 2000140.

(14) Operamolla, A.; Ragni, R.; Milano, F.; Tangorra, R. R.; Antonucci, A.; Agostiano, A.; Trotta, M.; Farinola, G. M. ″Garnishing″ the photosynthetic bacterial reaction center for bioelectronics. *J. Mater. Chem. C* **2015**, *3*, 6471−6478.

(15) Buscemi, G.; Vona, D.; Trotta, M.; Milano, F.; Farinola, G. M. Chlorophylls as Molecular Semiconductors: Introduction and State of Art. *Adv. Mater. Technol.* **2022**, *7*, 2100245.

(16) Nabiev, I.; Rakovich, A.; Sukhanova, A.; Lukashev, E.; Zagidullin, V.; Pachenko, V.; Rakovich, Y. P.; Donegan, J. F.; Rubin, A. B.; Govorov, A. O. Fluorescent Quantum Dots as Artificial Antennas for Enhanced Light Harvesting and Energy Transfer to Photosynthetic Reaction Centers. *Angew. Chem., Int. Ed.* **2010**, *49*, 7217−7221.
(17) Dutta, P. K.; Levenberg, S.; Loskutov, A.; Jun, D.; Saer, R.; Beatty, J. T.; Lin, S.; Liu, Y.; Woodbury, N. W.; Yan, H. A DNA-Directed Light-Harvesting/Reaction Center System. *J. Am. Chem. Soc.* **2014**, *136*, 16618−16625.
(18) Liu, J.; Mantell, J.; Jones, M. R. Minding the Gap between Plant and Bacterial Photosynthesis within a Self-Assembling Biohybrid Photosystem. *ACS Nano* **2020**, *14*, 4536−4549.
(19) Hassan Omar, O.; Gatta, S.; Tangorra, R. R.; Milano, F.; Ragni, R.; Operamolla, A.; Argazzi, R.; Chiorboli, C.; Agostiano, A.; Trotta, M.; Farinola, G. M. Synthetic Antenna Functioning As Light Harvester in the Whole Visible Region for Enhanced Hybrid Photosynthetic Reaction Centers. *Bioconjugate Chem.* **2016**, *27*, 1614−1623.
(20) Milano, F.; Tangorra, R. R.; Omar, O.; Ragni, R.; Operamolla, A.; Agostiano, A.; Farinola, G. M.; Trotta, M. Enhancing the Light Harvesting Capability of a Photosynthetic Reaction Center by a Tailored Molecular Fluorophore. *Angew. Chem.* **2012**, *124*, 11181−11185.
(21) la Gatta, S.; Milano, F.; Farinola, G. M.; Agostiano, A.; Donato, M.; Lapini, A.; Foggi, P.; Trotta, M.; Ragni, R. A highly efficient heptamethine cyanine antenna for photosynthetic Reaction Center: From chemical design to ultrafast energy transfer investigation of the hybrid system. *Biochim. Biophys. Acta, Bioenerg.* **2019**, *1860*, 350−359.
(22) Yaghoubi, H.; Li, Z.; Jun, D.; Lafalce, E.; Jiang, X.; Schlaf, R.; Beatty, J. T.; Takshi, A. Hybrid Wiring of the Rhodobacter sphaeroides Reaction Center for Applications in Bio-photoelectrochemical Solar Cells. *J. Phys. Chem. C* **2014**, *118*, 23509−23518.
(23) den Hollander, M. J.; Magis, J. G.; Fuchsenberger, P.; Aartsma, T. J.; Jones, M. R.; Frese, R. N. Enhanced photocurrent generation by photosynthetic bacterial reaction centers through molecular relays, light-harvesting complexes, and direct protein-gold interactions. *Langmuir* **2011**, *27*, 10282−10294.
(24) Friebe, V. M.; Millo, D.; Swainsbury, D. J. K.; Jones, M. R.; Frese, R. N. Cytochrome c Provides an Electron-Funneling Antenna for Efficient Photocurrent Generation in a Reaction Center Biophotocathode. *ACS Appl. Mater. Interfaces* **2017**, *9*, 23379−23388.
(25) Drepper, F.; Dorlet, P.; Mathis, P. Cross-linked electron transfer complex between cytochrome c(2) and the photosynthetic reaction center of Rhodobacter sphaeroides. *Biochemistry* **1997**, *36*, 1418−1427.
(26) Rosen, D.; Okamura, M. Y.; Abresch, E. C.; Valkirs, G. E.; Feher, G. Interaction of cytochrome c with reaction centers of Rhodopseudomonas sphaeroides R-26: localization of the binding site by chemical cross-linking and immunochemical studies. *Biochemistry* **1983**, *22*, 335−341.
(27) Ueno, T.; Hirata, Y.; Hara, M.; Arai, T.; Sato, A.; Miyake, J.; Fujii, T. Formation of Cross-Linked Complex of Photosynthetic Reaction-Center and Horse Heart Cytochrome-C - an Approach for Molecular-Organization with Cross-Linkage. *Mater. Sci. Eng., C* **1995**, *3*, 1−6.
(28) Usama, S. M.; Thavornpradit, S.; Burgess, K. Optimized Heptamethine Cyanines for Photodynamic Therapy. *ACS Appl. Bio Mater.* **2018**, *1*, 1195−1205.
(29) Pham, W.; Cassell, L.; Gillman, A.; Koktysh, D.; Gore, J. C. A near-infrared dye for multichannel imaging. *Chem. Commun.* **2008**, *16*, 1895−1897.
(30) Sissa, C.; Painelli, A.; Terenziani, F.; Trotta, M.; Ragni, R. About the origin of the large Stokes shift in aminoalkyl substituted heptamethine cyanine dyes. *Phys. Chem. Chem. Phys.* **2020**, *22*, 129−135.
(31) Peng, X.; Song, F.; Lu, E.; Wang, Y.; Zhou, W.; Fan, J.; Gao, Y. Heptamethine Cyanine Dyes with a Large Stokes Shift and Strong Fluorescence: A Paradigm for Excited-State Intramolecular Charge Transfer. *J. Am. Chem. Soc.* **2005**, *127*, 4170−4171.
(32) Axelrod, H. L.; Abresch, E. C.; Okamura, M. Y.; Yeh, A. P.; Rees, D. C.; Feher, G. X-ray structure determination of the cytochrome c(2): Reaction center electron transfer complex from Rhodobacter sphaeroides. *J. Mol. Biol.* **2002**, *319*, 501−515.
(33) Koepke, J.; Krammer, E.-M.; Klingen, A. R.; Sebban, P.; Ullmann, G. M.; Fritzsch, G. pH Modulates the Quinone Position in the Photosynthetic Reaction Center from Rhodobacter sphaeroides in the Neutral and Charge Separated States. *J. Mol. Biol.* **2007**, *371*, 396−409.
(34) Bushnell, G. W.; Louie, G. V.; Brayer, G. D. High-resolution three-dimensional structure of horse heart cytochrome c. *J. Mol. Biol.* **1990**, *214*, 585−595.
(35) Straley, S. C.; Parson, W. W.; Mauzerall, D. C.; Clayton, R. K. Pigment content and molar extinction coefficients of photochemical reaction centers from Rhodopseudomonas spheroides. *Biochim. Biophys. Acta* **1973**, *305*, 597−609.
(36) Margoliash, E.; Frohwirt, N. Appendix—Spectrum of horse-heart cytochrome c. *Biochem. J.* **1959**, *71*, 570−572.
(37) Buscemi, G.; Milano, F.; Vona, D.; Farinola, G. M.; Trotta, M. Effect of chemical substitution on the surface charge of the photosynthetic Reaction Center from Rhodobacter sphaeroides: an in-silico investigation. *MRS Adv.* **2020**, *5*, 2309−2316.
(38) Williams, J. C.; Steiner, L. A.; Feher, G. Primary structure of the reaction center from Rhodopseudomonas sphaeroides. *Proteins* **1986**, *1*, 312−325.
(39) Feher, G. Some chemical and physical properties of a bacterial reaction center particle and its primary photochemical reactants. *Photochem. Photobiol.* **1971**, *14*, 373−387.
(40) Rath, A.; Glibowicka, M.; Nadeau, V. G.; Chen, G.; Deber, C. M. Detergent binding explains anomalous SDS-PAGE migration of membrane proteins. *Proc. Natl. Acad. Sci.* **2009**, *106*, 1760−1765.
(41) Kleinfeld, D.; Okamura, M. Y.; Feher, G. Electron transfer in reaction centers of Rhodopseudomonas sphaeroides. II. Free energy and kinetic relations between the acceptor states QA−QB− and QAQ2−B. *Biochim. Biophys. Acta* **1985**, *809*, 291−310.
(42) Buscemi, G.; Vona, D.; Ragni, R.; Comparelli, R.; Trotta, M.; Milano, F.; Farinola, G. M. Polydopamine/Ethylenediamine Nanoparticles Embedding a Photosynthetic Bacterial Reaction Center for Efficient Photocurrent Generation. *Adv. Sustainable Syst.* **2021**, *5*, 2000303.
(43) Milano, F.; Ciriaco, F.; Trotta, M.; Chirizzi, D.; Leo, V.; Agostiano, A.; Valli, L.; Giotta, L.; Guascito, M. R. Design and modelling of a photo-electrochemical transduction system based on solubilized photosynthetic reaction centres. *Electrochim. Acta* **2019**, *293*, 105−115.
(44) Isaacson, R. A.; Lendzian, F.; Abresch, E. C.; Lubitz, W.; Feher, G. Electronic structure of Q-A in reaction centers from Rhodobacter sphaeroides. I. Electron paramagnetic resonance in single crystals. *Biophys. J.* **1995**, *69*, 311−322.
(45) Milano, F.; Agostiano, A.; Mavelli, F.; Trotta, M. Kinetics of the quinone binding reaction at the Q(B) site of reaction centers from the purple bacteria Rhodobacter sphaeroides reconstituted in liposomes. *Eur. J. Biochem.* **2003**, *270*, 4595−4605.

https://doi.org/10.1021/acs.bioconjchem.2c00527
Bioconjugate Chem. 2023, 34, 629−637